

## On the Less Known Effects of Environment and Specimen Geometry on Creep Fracture of Nickel Alloys

M.C. Pandey and P. Rama Rao

*Defence Metallurgical Research Laboratory, Hyderabad-500 258*

### ABSTRACT

Attention has been drawn to the fact that during exposure of nickel to air at elevated temperatures, oxygen diffuses through the grain boundary and reacts with carbon forming gas bubbles of carbon monoxide and/or carbon dioxide. Voids are produced due to the high pressure generated by the gas bubbles which cause creep embrittlement. Alloying nickel with 3.8 weight per cent aluminium, which is a stronger oxide forming element as compared to carbon, could not prevent diffusion of oxygen during exposure of the alloy to air at elevated temperatures. The diffusing oxygen reacts even in the *Ni-Al-C* system, with carbon and forms gas bubbles of *CO* and *CO<sub>2</sub>*, which lead to creep embrittlement. The presence of 15 weight per cent chromium in nickel (Inconel 600 and Inconel alloy X-750), however, plays an interesting role on the kinetics of oxygen diffusion. At temperatures 1050 °C and below, during exposure to air at atmospheric pressure, oxygen can diffuse along the grain boundary and reacts with carbon forming gas bubbles of carbon monoxide, where as at 1120 °C and above, the formation of 'barrier' oxide scale, chromium oxide, at the surface prevents diffusion of oxygen. On the other hand, the presence of chromium, as observed in Inconel alloy X-750, does not play an effective role in preventing diffusion of oxygen along the grain boundary in poor vacuum. Circumstantial evidence suggests that diffusing oxygen reacts with carbon and forms gas bubbles of *CO* with consequential creep embrittlement, reduction in creep life and enhancement in creep rate. It has been shown that exposure of the alloy in poor vacuum has a much more damaging effect on the creep properties than that of an atmospheric pressure. It is, therefore, emphasized that exposure of nickel base superalloys to poor vacuum at elevated temperatures must

be avoided; in particular this effect is more pronounced in the alloy with thin section size. It is also shown that even in the absence of oxygen interaction *prior* to creep testing, section size has considerable influence on the creep properties which is believed to be caused by oxygen interaction *during* creep deformation. For the same section size, the creep properties may be different in specimens of different geometries. But for the same ratio of cross-sectional area to perimeter ( $A/P$ ), rupture lifetime becomes independent of specimen geometry. Failure analysis of an aero engine blade has been presented as a case study to emphasize that while designing a component, utmost care must be exercised to avoid thin sections.

## 1. INTRODUCTION

It was my (PRR) great privilege to have had the opportunity to work at the Indian Institute of Science, Bangalore, during the period Professor S. Bhagavantam was its illustrious Director. Even though at the bottom rung of the Faculty ladder, I was fortunate to come into contact with one occupying the highest office at the Institute. What made this possible was the genial and generous personality of late Dr. Bhagavantam. My receiving help from him directly in my research at this stage shall remain an unforgettable experience. There were also numerous occasions when youngsters like me (then) could listen to him lecture at the Institute. Endowed as he was with a rare gift of lecturing, the impact that Professor Bhagavantam made through his discourses has endured. And I can go on. I feel so good and greatly privileged to have been asked to contribute to this Special Issue of Defence Science Journal.

Aero engines constitute an excellent example of a major modern technological system, not only from an engineering design viewpoint, but also in terms of advanced materials designed to enable components such as engine blades, perform under severe environmental conditions of temperature, stress and hot corrosive gases. Nickel base superalloys have come to be established as the most viable metallic materials for such applications. There is a considerable volume of information available in the literature in regard to the role of alloy chemistry and microstructures, on the basis of which substantial understanding of their mechanical behaviour and performance has emerged. Even so, there are issues which are yet to be clarified. The present paper addresses some of these like the effect of oxygen interaction with the system implying not only the basic materials, but also the way the component is shaped in terms of section size and geometry. It is interesting to point out that although the phenomenon we will be concerned with in one sense is a rather simple process pertaining to the influence of oxygen, it has interesting technological implications. Prof. Bhagavantam, during the course of his long and illustrious career, demonstrated, by his own example, the importance of bridging science and engineering, and it is within this framework that the present work has been attempted to be carried out. Thus, we have felt that in order to understand the combined effect of environment and creep during service of a gas turbine engine component of a complex nickel base superalloy, we should develop progressive levels of understanding starting from the base metal. Accordingly, we present here a summary of our work over a number of years covering four materials, namely,

- (i) Commercially pure nickel with 0.03 wt per cent carbon,
- (ii) A single phase nickel-aluminium (3.8 wt per cent)–carbon (0.09 wt per cent) alloy,
- (iii) A single phase high temperature commercial nickel alloy, Inconel 600, containing 15 wt per cent chromium, 9 wt per cent iron and 0.06 wt per cent carbon, and
- (iv) A complex commercial high temperature nickel base superalloy, Inconel X-750, containing 15 wt per cent chromium, 7.1 wt per cent iron, 2.5 wt per cent titanium, 0.68 wt per cent aluminium, 0.90 wt per cent niobium and 0.03 wt per cent carbon.

In the case of the alloy Inconel X-750, we have also brought into consideration the effect of section size in three specimen geometries and this work has a bearing on the engineering design of engine components.

## 2. EFFECT OF OXYGEN INTERACTION

### 2.1 Commercially Pure Nickel

Nickel, being the base metal of nickel base superalloys, has been studied in great detail. Early work showed that heating of nickel in air at elevated temperatures led to the formation of voids along grain boundaries<sup>1-4</sup>. It was postulated that nickel being a metal deficient oxide, vacancies form during oxidation. Accumulation of these vacancies led to the formation of voids<sup>5</sup>. Build up of stresses at the oxide-metal interface was considered to be another factor responsible for the formation of voids. Some researchers suggested that reaction between diffusing oxygen and carbon in the nickel metal led to the formation of carbon monoxide gas which resulted in voids along the grain boundary<sup>6,7</sup>. A more comprehensive work providing better understanding of the oxidation behaviour of nickel has been carried out by Bricknell and Woodford<sup>8,9</sup> who have shown that voids along the grain boundary are produced due to the formation of carbon dioxide gas bubbles. Our own work in nickel has shown voids along the grain boundary (Fig. 1). Figure 2, from the work of Iacocca and Woodford<sup>10</sup>, shows the depth of such voids produced as a function of exposure time and temperature. Exposure of nickel in an environment containing oxygen at a partial pressure of about  $10^{-6}$  Pa at 1000 °C led to the formation of voids. Raj<sup>11</sup> and Dyson<sup>12</sup> have shown theoretically that pressure generated by the production of carbon monoxide and carbon dioxide is quite adequate to plastically deform the grain boundary containing these gases (Fig. 3). The voids produced in nickel in the near surface region reduces the load bearing cross-sectional area thereby weakening the material. During creep-testing, the voids grow, interlink and form single and multiple grain facet cracks which generate a notch effect resulting in poor ductility.

During exposure of nickel to air at elevated temperatures, in addition to voids along the grain boundary of the base metal, nickel oxide forms at the surface (Fig. 1). We have observed that oxide scale of 50  $\mu\text{m}$  thickness forming on a 3 mm diameter specimen leads to considerable creep strengthening whereas the presence of voids along the grain boundary causes creep weakening, embrittlement and reduced life

(Fig. 4). Similar creep behaviour has been observed at other stresses as well. It is believed that creep strengthening is caused due to the build up of dislocations at the oxide-metal interface as the dislocations generated during creep cannot escape from the surface due to the presence of the oxide scale.

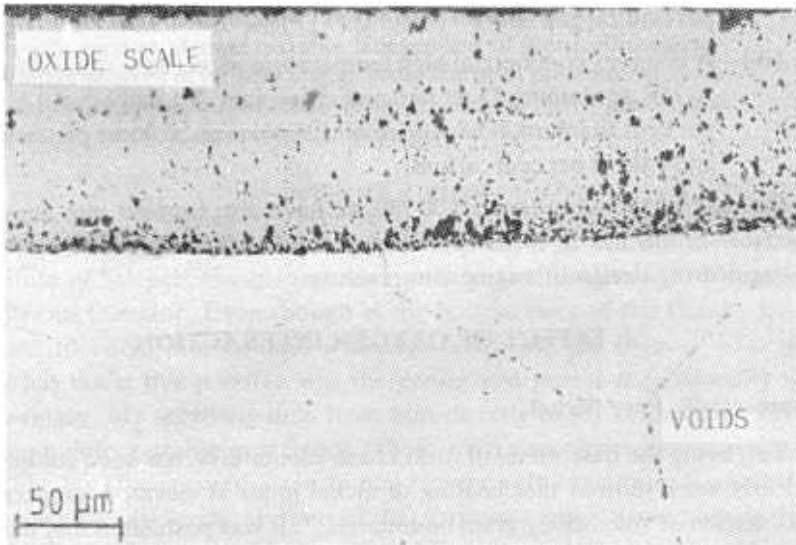


Figure 1. Voids produced along grain boundary of nickel after exposure to air at 1050 °C for 48 h.

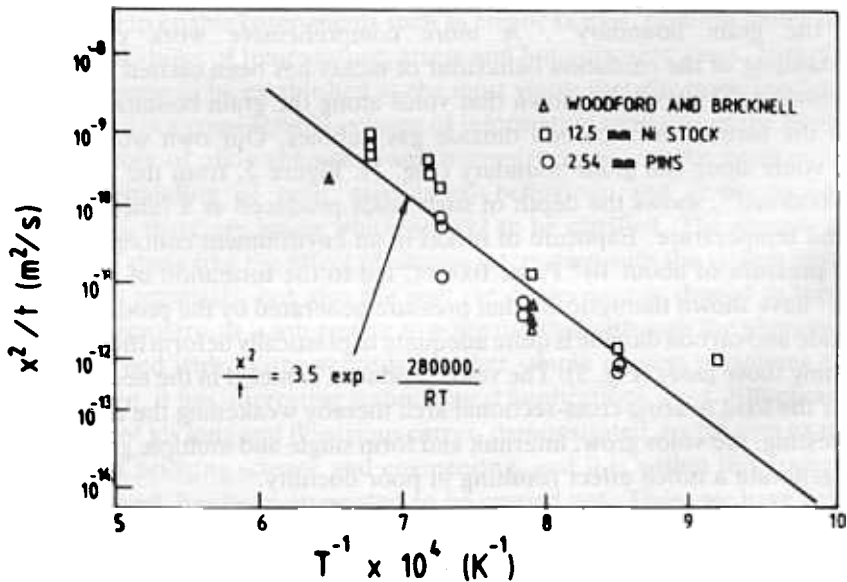


Figure 2. Depth of voids ( $x$ ), as a function of exposure time ( $t$ ), and temperature ( $T$ ), in a commercially pure nickel<sup>10</sup>.

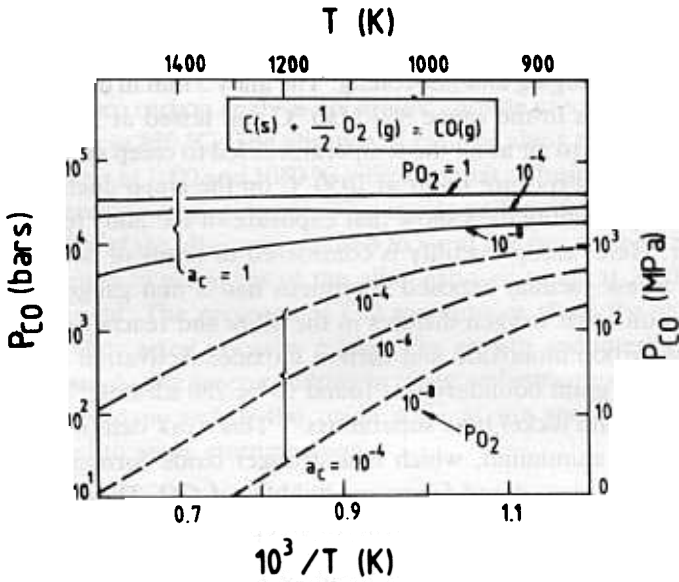


Figure 3. Partial pressure of carbon monoxide generated during oxidation in an oxygen environment at different pressures. It can be shown that the pressure generated by  $CO_2$  will be higher than that of  $CO$  gas.  $a_c$  is carbon activity.

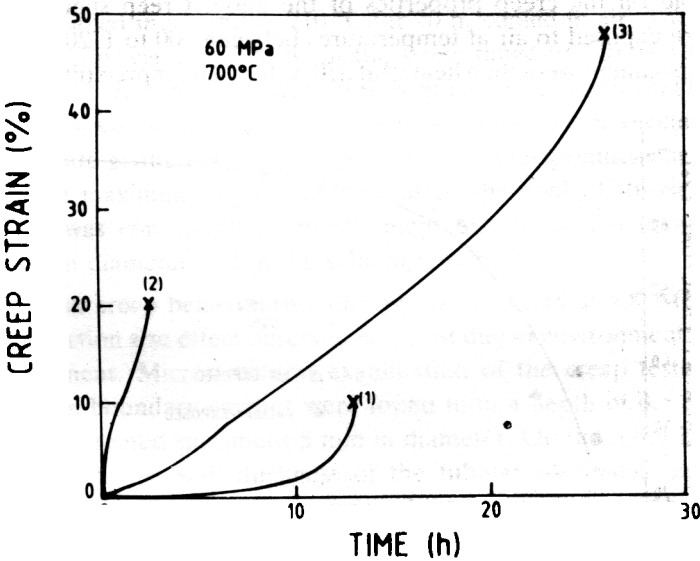


Figure 4. Effect of oxide scale and voids produced during oxidation of nickel at 1050 °C for 11 h on the creep behaviour at 700 °C and 60 MPa. Curve 1 represents the oxidized specimen with oxide scale, curve 2, the oxidized specimen without oxide scale (oxide scale thickness, 50  $\mu$ m, was removed by emery paper), and curve 3, the deformation behaviour of creep specimen 3 mm in diameter heated in a bar form (8 mm diameter) in an evacuated sealed quartz tube along with the other two specimens.

## 2.2 Nickel-Aluminium-Carbon Alloy

The alloy is a single phase wrought alloy, manufactured by vacuum induction melting followed by forging and hot-rolling. The alloy 5 mm in diameter, was exposed to air at temperatures in the range 860-1150 °C and tested at 700 °C and 100 MPa. Exposure of the alloy to air at all the temperatures led to creep embrittlement. Figure 5 shows the effect of exposure to air at 1050 °C on the creep ductility of the alloy at 700 °C. The creep ductility data show that exposure of the alloy to air leads to creep embrittlement. Here, creep ductility is considered in terms of percentage reduction of area since a few vacuum exposed specimens had 3 mm gauge diameter. In this study, it was found that oxygen diffuses in the alloy and reacts with carbon forming gas bubbles of carbon monoxide and carbon dioxide. Activation energy for oxygen diffusion along the grain boundary was found to be 280 kJ/mole<sup>13</sup> which is the same as in pure nickel<sup>10</sup> and nickel base superalloys<sup>14</sup>. This work demonstrates that inspite of the presence of aluminium, which is a stronger oxide forming element, carbon reacts with diffusing oxygen and forms gas bubbles of CO. These gas bubbles act as cavity nuclei, as found in nickel, and lead to creep embrittlement.

## 2.3 Inconel Alloy 600

This is a single phase wrought nickel base superalloy and is being extensively used at elevated temperatures in an oxidizing environment since it is believed that due to the presence of chromium its properties are not degraded in such environment. However, our recent work<sup>15,16</sup> has shown that exposure temperature plays the most significant role on the creep properties of the alloy. Creep specimens 3.5 mm in diameter were exposed to air at temperatures between 900 to 1120 °C for 150 h. The air-exposed specimens were then heated at 850 °C for 24 h for precipitation of chromium

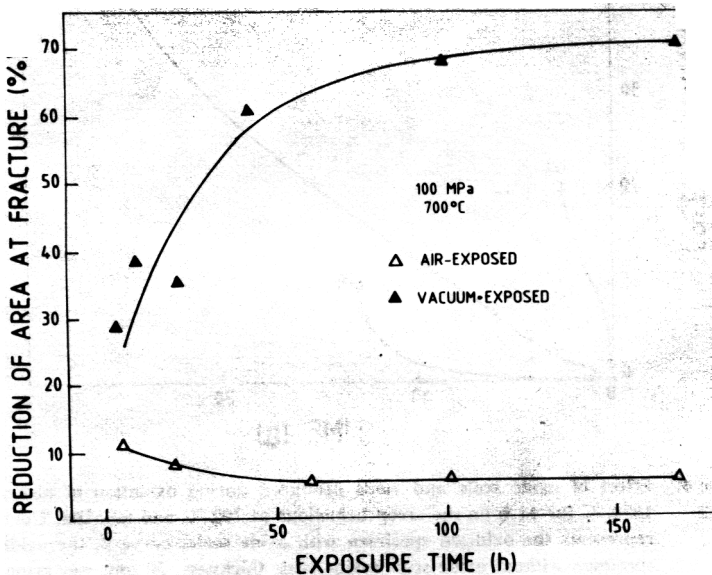


Figure 5. Effect of oxidation at 1050 °C on the creep ductility of Ni-Al-C alloy tested at 700 °C and 100 MPa.

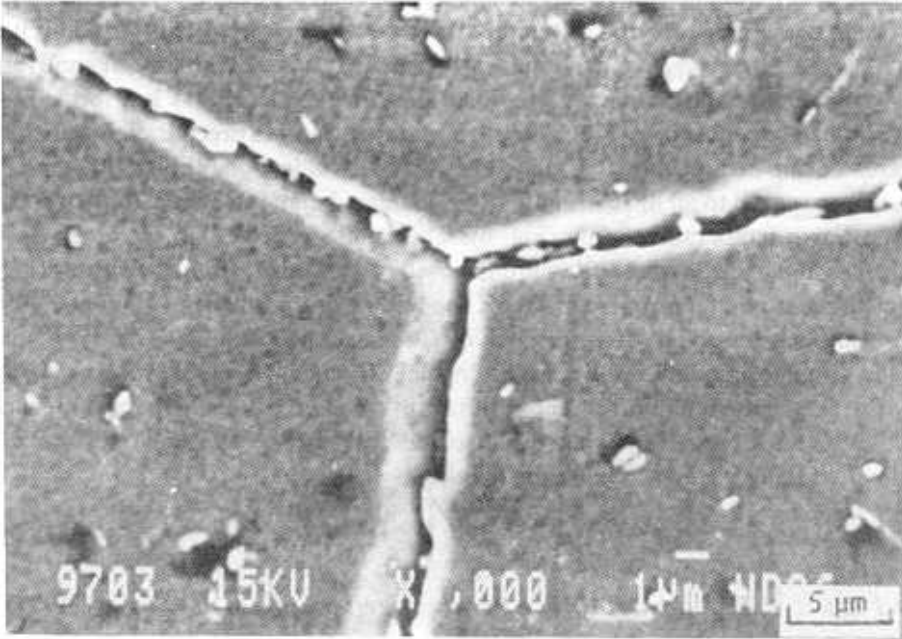
carbide along the grain boundary. Heating at 850 °C was done to examine whether diffusion of oxygen occurred at temperatures between 900 and 1120 °C and if it is so whether diffusing oxygen reacted with carbon at the exposure temperatures and formed gas bubbles of carbon monoxide and carbon dioxide. If CO gas has formed as we have shown via the Leco carbon analysis apparatus, carbide precipitation will not take place<sup>17</sup> during heating at 850 °C. The absence of carbide along the grain boundary of the alloy exposed to air at 1000 and 1050 °C indicated that diffusion of oxygen occurred at these two temperatures only (Fig. 6). This is also reflected on the creep ductility at 727 °C and 75 MPa of the alloy pre-exposed to air at the two temperatures (Fig. 7). Considerable reduction in creep life of the alloy exposed to air at 1000 and 1050 °C has also been observed. The presence of CO gas bubbles along the grain boundary of the air-exposed alloy acted as cavity nuclei. The growth and interlinkage of these cavity nuclei occurred during creep resulting in creep embrittlement and poor rupture lifetime<sup>18</sup>. As observed in nickel, the oxide scale at the specimen surface of the air-exposed alloy led to creep strengthening.

## 2.4 Inconel Alloy X-750

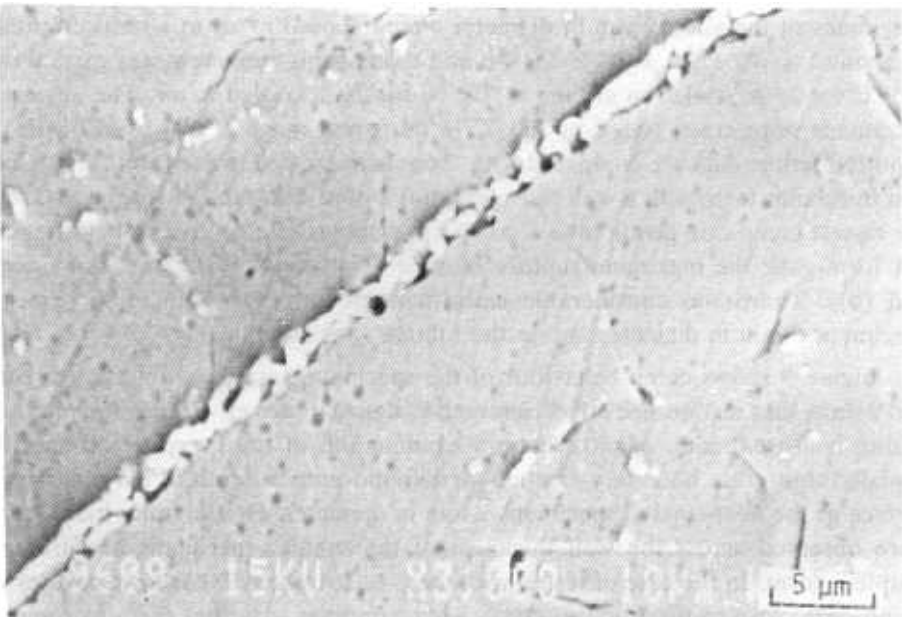
### 2.4.1 Effect of Exposure to Air at a Reduced Pressure of $2 \times 10^{-2}$ Pa at 1150 °C

The material is a complex gamma prime strengthened wrought nickel base superalloy. Pandey *et al.*<sup>19-21</sup> have studied the effect of air-pressure, exposure time and temperature on the creep behaviour of the alloy. In the first set of experiments, specimens of the alloy 5 mm in diameter were exposed to air at a reduced pressure of about  $2 \times 10^{-2}$  Pa at 1150 °C for 4 h and then ageing treatment was carried out at 845 °C for 24 h, cooled in air and at 710 °C for 20 h, cooled in air. The air-exposed specimens were creep tested at 700 °C in the stress range of 240 to 610 MPa. The rupture lifetime data are compared with those heat-treated in bar form (12 × 12 mm) and in tubular form with a wall thickness of 0.8 mm. The tubular specimens crept at the fastest creep rate giving lowest creep life whereas, the specimens heat-treated in bar form gave the maximum rupture lifetime at all the applied stresses (Figs. 8(a) and (b)). There was considerable embrittlement observed both in the machined specimens 5 mm in diameter and in the tubular specimens.

Figure 9 shows creep behaviour of the specimens tested at 400 MPa. Figures 8 and 9 show that section size effect observed is almost due to environmental interaction during heat-treatment. Microstructural examination of the creep tested specimens revealed that grain boundary cavities were found upto a depth of 0.5 mm from the surface of the heat-treated specimens 5 mm in diameter. On the other hand, cavities were observed across the wall thickness of the tubular specimens heat-treated in testpiece form. In the case of tested specimens heat-treated in bar form cavities were found only close to the fracture end<sup>19</sup>. These findings indicated that environmental interaction during heat-treatment led to the formation of cavities. Growth and interlinkage of these cavities occurred during creep-testing. Since duration of heat-treatment was only 4 h, environmental interaction leading to cavitation was limited upto a depth of 0.5 mm from the surface of the specimens 5 mm in diameter. In the case of tubular specimens, heat-treated in test-piece form, environmental



(a)



(b)

**Figure 6.** (a) The absence of carbide along the grain boundary of the alloy exposed to air at 1050 °C for 150 h and followed by ageing at 850 °C for 24 h, suggesting that diffusion of oxygen occurred and reacted with carbon leading to the formation of CO gas<sup>7</sup>. (b) The same treatment in vacuum, showing the presence of carbide.

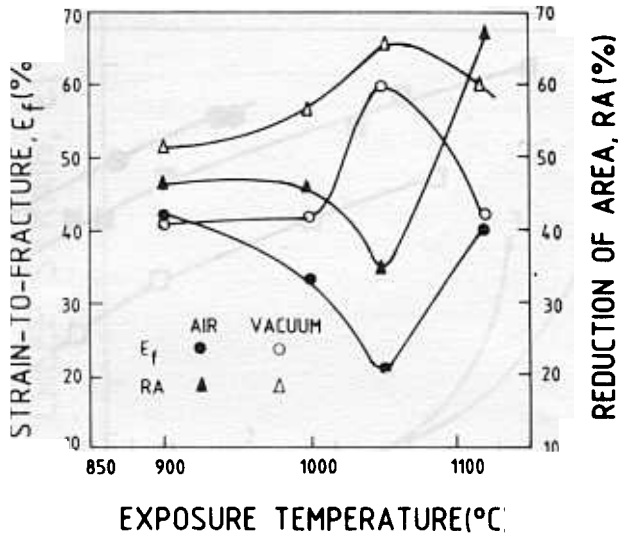
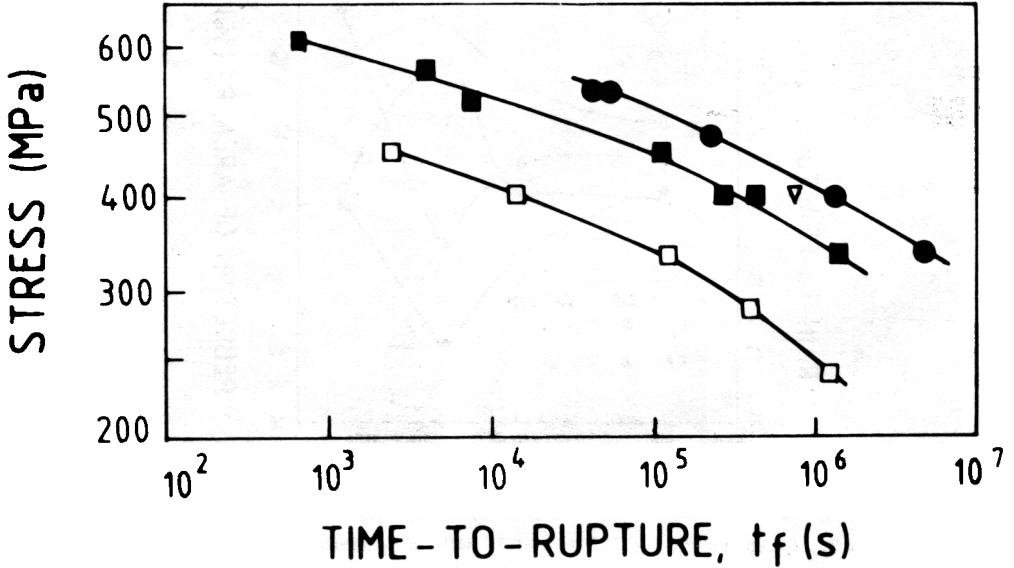


Figure 7. Creep ductility at 727 °C and 75 MPa of specimens exposed to air and vacuum for 150 h at various temperatures.

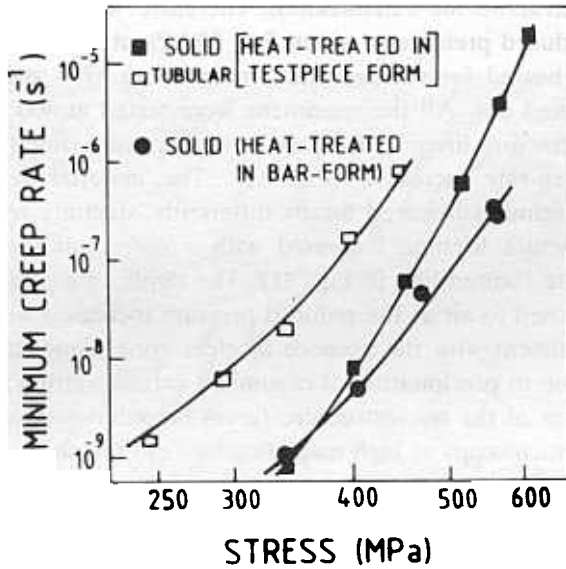
interaction could occur from both sides of the wall of 0.8 mm thickness and hence cavitation was found across the wall thickness. Therefore, to study the effect of heating time in air at a reduced pressure of about  $2 \times 10^{-2}$  Pa at 1150 °C, specimens 5 mm in diameter were heated for various times from 0.5 to 67 h and then the ageing treatment was carried out. All the specimens were tested at 400 MPa and 700 °C. The ductility and fracture lifetime decreased with exposure time (Fig. 10) whereas, the minimum creep-rate increased (Fig. 11). The material heat-treated before manufacture of specimens behaved totally differently, ductility remained relatively constant while fracture lifetime increased with a corresponding decrease in the minimum creep-rate (dotted line in Fig. 11). The depth of cavitation in the tested specimens pre-exposed to air at the reduced pressure increased with exposure time. This was also consistent with the absence of clear zone along the grain boundary which is formed due to precipitation of chromium carbide during ageing treatment. In fact, examination of the microstructure (grain boundary without clear zone) by scanning electron microscopy at high magnifications did not show any carbide along the grain boundary. This provides circumstantial evidence that during exposure to air at the reduced pressure at 1150 °C, diffusion of oxygen occurred and reacted with carbon forming gas bubbles of CO or/and CO<sub>2</sub>. The gas bubbles led to the formation of cavity nuclei whose growth and interlinkage during creep led to creep embrittlement and reduced fracture lifetime. The decrease in creep resistance with time of prior exposure has been modelled very accurately using physically-based Kachanov-type coupled differential equations<sup>22</sup>.

#### 2.4.2 Exposure of Inconel Alloy X-750 to Air at Atmospheric Pressure at 1150 °C

In this section, it is shown that exposure of the alloy Inconel X-750 to air (at atmospheric pressure) at 1150 °C does not cause creep embrittlement. In this study, specimens 5 mm in diameter were exposed to air at atmospheric pressure at 1150 °C



(a)



(b)

Figure 8. A comparison of (a) creep life, and (b) minimum creep rate at 700 °C between heat-treated in (1) bar form (●), (2) specimen form 5mm in diameter (■), and (3) tubular specimen with wall thickness of 0.8 mm in (i) test-piece form (□), and (ii) bar form (▽), at a reduced pressure of about  $2 \times 10^{-2}$  Pa.

for times ranging from 4 to 120 h and were given ageing treatment as described in the previous section. Clear zones and chromium carbide precipitates were observed along the grain boundary. Further, creep-testing at 700 °C and 400 MPa of the pre-exposed specimens did not show any embrittling effect (Fig. 12). This study thus

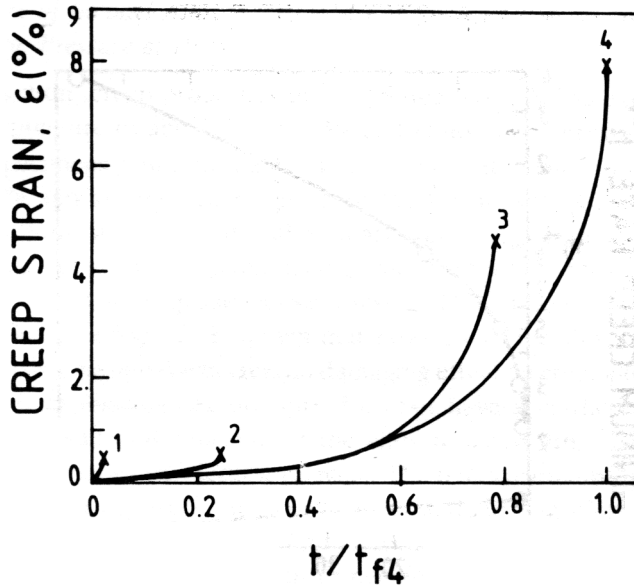


Figure 9. An example of the dramatic effect of heat-treatment at a reduced air pressure of about  $2 \times 10^{-2}$  Pa at 1150 °C on creep behaviour of Inconel alloy X-750 at 700 °C and 400 MPa. (1) Tubular specimen (heat-treated in specimen form), (2) solid specimen 5 mm in diameter (heat-treated in specimen form), (3) tubular specimen (heat-treated in bar form), and (4) solid specimen (5 mm diameter, heat-treated in bar form). Lifetime data ( $t$ ), is normalized with respect to  $t_{f4}$ , the time taken to rupture specimen number 4.

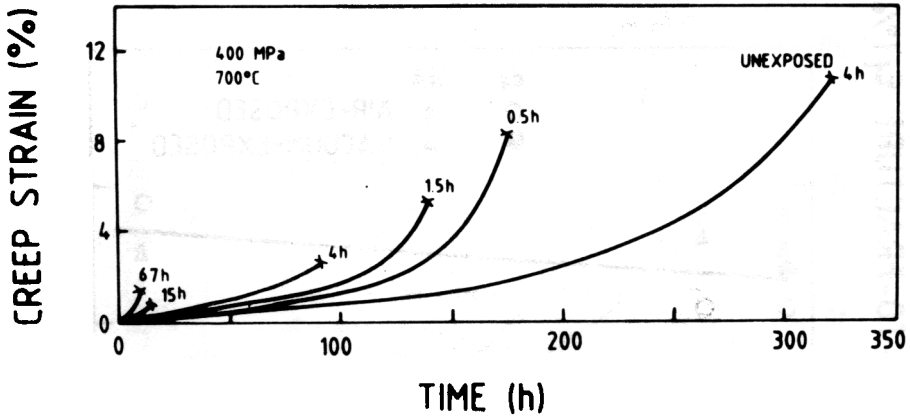


Figure 10. Creep behaviour at 700 °C and 400 MPa of Inconel alloy X-750 heated for various times (0.5 to 67 h) in air at a reduced pressure of  $2 \times 10^{-2}$  Pa at 1150 °C. The unexposed specimen was heated for 4 h in bar form (12 mm diameter) and then machined to 5 mm diameter.

provides circumstantial evidence that diffusion of oxygen did not occur along the grain boundary during exposure to air (at atmospheric pressure) at 1150 °C unlike in the air at a reduced pressure of about  $2 \times 10^{-2}$  Pa.

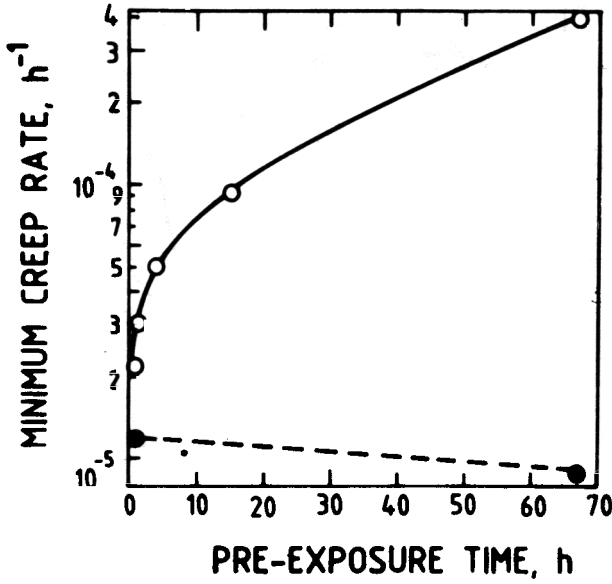


Figure 11. Minimum creep rate versus exposure time (data taken from creep curves shown in Fig. 10). Data represented by the dotted line is for the specimens heat-treated in bar form in air.

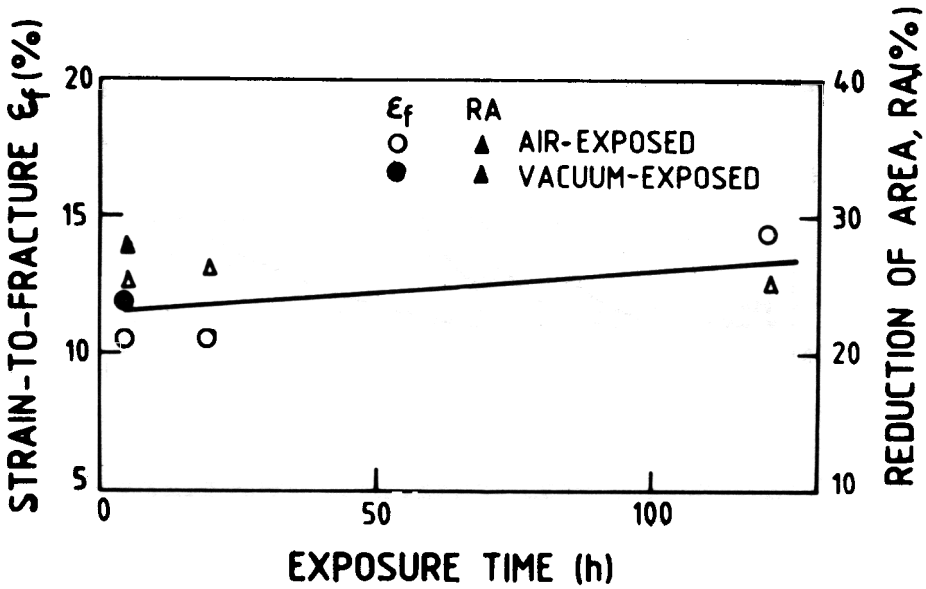


Figure 12. Creep ductility at 700 °C and 400 MPa of Inconel alloy X-750 exposed to air at atmosphere pressure at 1150 °C.

### 2.4.3 Exposure of Inconel Alloy X-750 to Air at Reduced Pressure of $2 \times 10^{-2}$ Pa and at Atmospheric Pressure at 1050 °C

In this section, creep properties of the Inconel alloy X-750 exposed to air both at a reduced pressure of about  $2 \times 10^{-2}$  Pa and atmospheric pressure at 1050 °C are presented. Specimens 5 mm in diameter were exposed to air at a reduced pressure of  $2 \times 10^{-2}$  Pa and at atmospheric pressure for 4 h at 1050 °C. One specimen was heated in bar form in evacuated sealed quartz tube for 4 h in air at 1050 °C. The three specimens were further given ageing treatment as per the schedule described in Section 2.4.1. The three specimens were tested at 700 °C and 400 MPa. Their creep behaviour is shown in Fig. 13. It is seen that exposure of the alloy to air at a reduced pressure of  $2 \times 10^{-2}$  Pa had the maximum damaging effect on creep properties, whereas exposure to air at atmospheric pressure does not have a marked effect. However, further study showed that exposure of the alloy to air at atmospheric pressure for longer periods did cause considerable damage. The fracture lifetime and creep ductility both decreased with exposure time (Figs. 14(a) and (b)). Depletion of carbide was observed near the specimen surface. This confirms our earlier finding in Inconel 600 that diffusion of oxygen occurs only in a specific temperature regime (Section 2.3). It was also found that diffusion of oxygen occurred beyond the carbide depleted region and presence of this oxygen alone led to creep embrittlement. Dyson and Osgerby<sup>18</sup> have also shown that exposure of the alloy to air (atmospheric pressure) at 1000 °C leads to creep embrittlement.

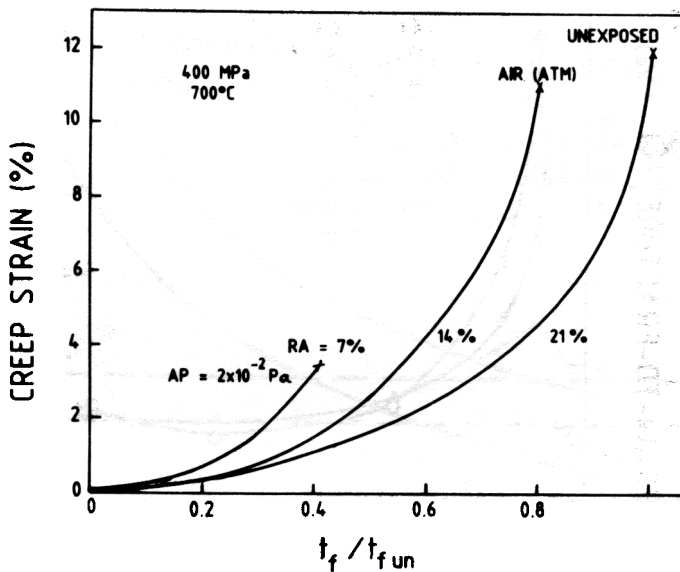
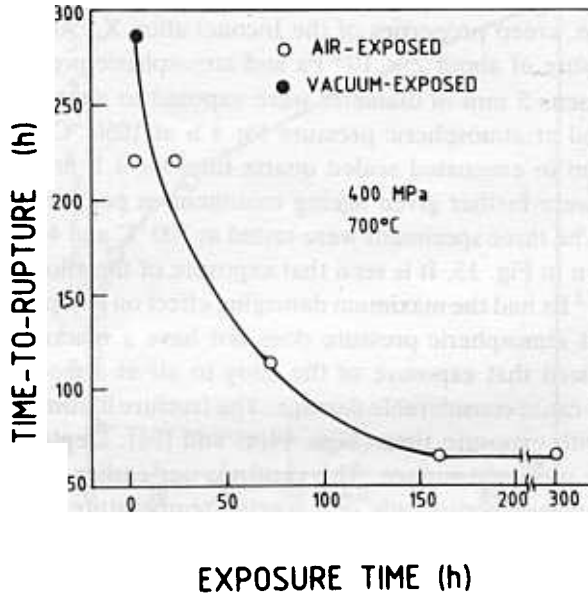
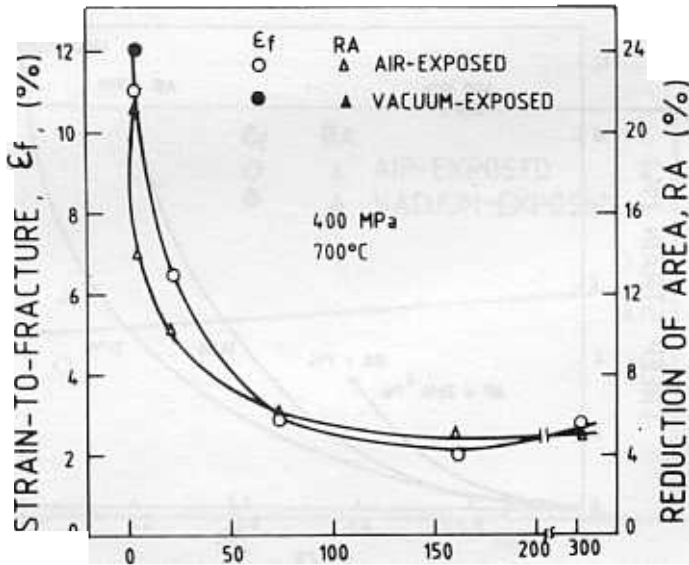


Figure 13. Creep behaviour at 700 °C and 400 MPa of Inconel alloy X-750 heated at 1050 °C for 4 h in air (1) at a reduced pressure of  $2 \times 10^{-2}$  Pa, (2) at atmospheric pressure, and (3) unexposed heated in the evacuated sealed quartz tube.



(a)



(b)

Figure 14. (a) Fracture lifetime, and (b) creep ductility at 700 °C and 400 MPa as a function of exposure time in air at atmospheric pressure at 1050 °C.

### 3. MECHANISM OF OXYGEN DIFFUSION IN INCONEL 600 AND INCONEL ALLOY X-750

Creep data obtained in Inconel 600 and Inconel alloy X-750 suggest that exposure temperature and air pressure play the most important role on the kinetics of oxygen diffusion along the grain boundary. The effect of exposure temperature on the creep properties has been addressed in our earlier publication<sup>15</sup>. It seems<sup>15,18</sup> that there are two competing mechanisms which dictate whether diffusion of oxygen along the grain boundary can occur or not, namely, (a) formation of a 'barrier' oxide scale, and (b) diffusion of oxygen into the alloy along the grain boundary. At low oxygen partial pressure ( $\sim 10^{-2}$  Pa) at 1050 and 1150 °C the formation of a barrier oxide scale  $Cr_2O_3$  in Inconel alloy X-750) is delayed and therefore, oxygen can diffuse along the grain boundary and react with carbon forming gas bubbles of carbon monoxide which act as cavity nuclei. At atmospheric air pressure at 1150 °C, any oxygen available at the surface immediately reacts with chromium already diffused towards the surface, and forms impervious layer of chromium oxide. The concentration of oxygen at the chromium oxide-metal interface will be so low that carbon cannot react with oxygen. However, if exposure temperature is such (1000 and 1050 °C in Inconel alloy X-750) that the formation of chromium oxide, which acts as a barrier to oxygen diffusion, is delayed and thus oxygen can diffuse through the grain boundary and form gas bubbles of carbon monoxide. A schematic diagram illustrating these features is shown in Fig. 15 which demonstrates that at a reduced air pressure of  $10^{-2}$  Pa, the depth of oxygen diffusion is dependent on temperature whereas, at atmospheric pressure, diffusion of oxygen will be suppressed at  $T_2$  (1120 °C in Inconel 600, and 1150 °C in

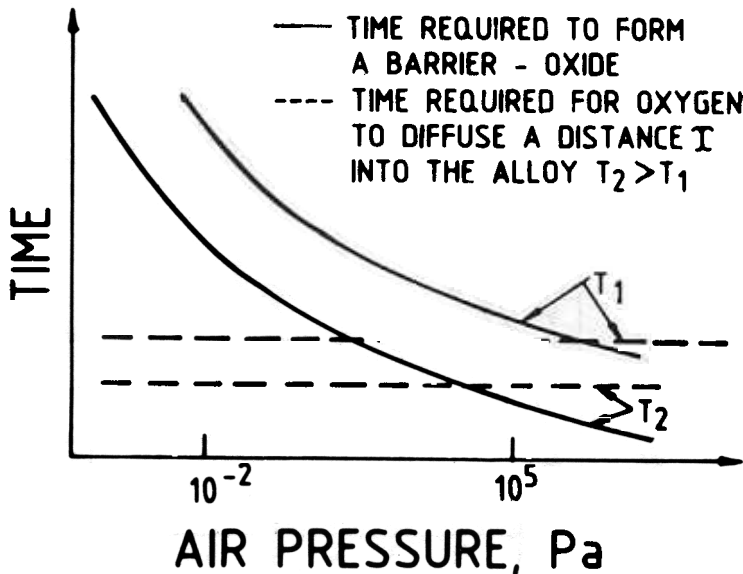


Figure 15. Schematic diagram illustrating possible mechanistic explanation of different effects of temperature on the extent of oxygen interaction at different oxygen partial pressures<sup>18</sup>.

Inconel alloy X-750), because the barrier oxide forms too quickly. At the lower temperature  $T_1$  (1000 and 1050 °C in both Inconel 600 and Inconel alloy X-750), the higher activation energy of barrier oxide formation ensures that oxygen can diffuse freely. Dyson and Osgerby<sup>18</sup> have also referred to oxygen diffusion through the surface scale by short-circuit diffusion—either through fissures or along oxide grain boundaries. The nature of oxide scale will depend upon the exposure temperature and oxygen partial pressure.

#### 4. EFFECT OF SECTION SIZE AND SPECIMEN GEOMETRY ON CREEP LIFE

It has been shown in the preceding sections that environmental interaction during heat-treatment of Inconel alloy X-750 can lead to a significant section size effect on the creep life. Section size effect has been observed in many nickel base superalloys even though environmental interaction did not take place during heat-treatment<sup>17,22,23</sup>. It is believed to be due to environmental interaction during creep-testing, although little experimental evidence is available.

In a recent publication<sup>24</sup> the combined effect of section size and specimen geometry on the creep and creep fracture behaviour of Inconel alloy X-750 was addressed. Design engineers encounter practical problems when using the laboratory creep data. It has been customary to consider fracture lifetime data of round specimens or in some cases flat specimens of equivalent thickness to that of the component. The effect of section size for three specimen geometries is shown in Fig. 16. It is seen that creep life decreases with decreasing section size and is the lowest in the round specimen at a given section size. It is important to note that in the case of round specimen, there is only one parameter—diameter (or section size); therefore, creep life can be directly

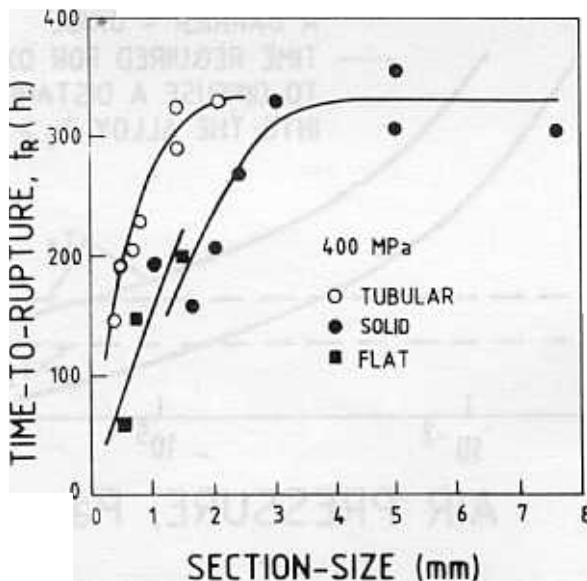


Figure 16. Time-to-pressure at 700 °C and 400 MPa as a function of section size of round, flat and tubular specimens of Inconel alloy X-750.

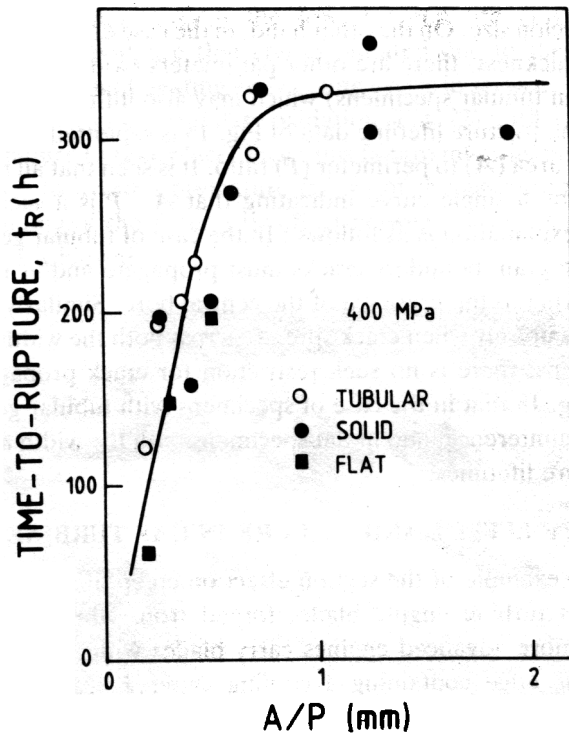
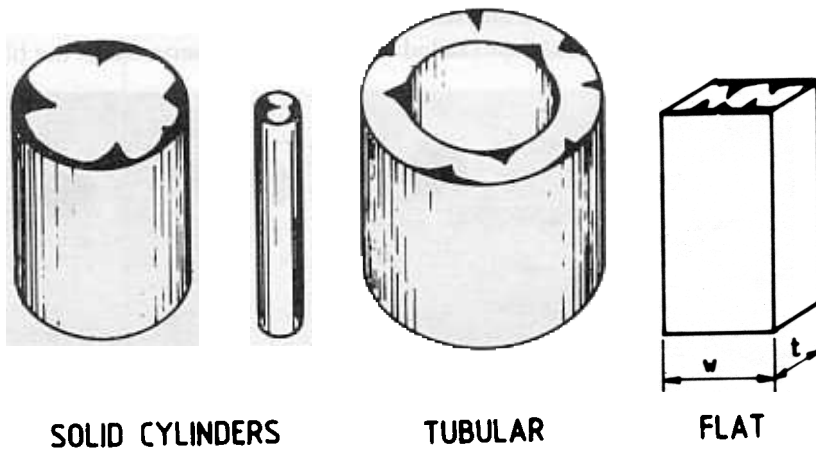


Figure 17. Time-to-rupture data shown in Fig. 16 is replotted as a function of the ratio of the cross-sectional area ( $A$ ) to the perimeter ( $P$ ).



**AREA DAMAGED BY GRAIN BOUNDARY CRACKING**

Figure 18. Schematic diagram showing the extent of cross-sectional area damaged due to grain boundary cavitation and the role of the perimeter in specimens of the three geometries during creep.

linked with the section size. On the other hand, in the case of flat and tubular specimens, besides section thickness, there are other parameters (width in flat, and internal and outer diameters in tubular specimens) which may also influence the fracture lifetime. In view of this, the fracture lifetime data of Fig. 15 is replotted in Fig. 17 as a function of cross-sectional area ( $A$ ) to perimeter ( $P$ ) ratio. It is seen that all the fracture lifetime data is denoted by a single curve indicating that  $A : P$  is a successful normalizing parameter. Our explanation is as follows : In the case of tubular geometry, for failure to take place, the grain boundary cracks must propagate and/or interlink across the circumference owing to the presence of the central bore. Similarly, in flat specimens, separation will occur only when crack spreads across both the width and the thickness. In round specimens, there is no such restriction for crack propagation (Fig. 18). It can be seen in Fig. 18 that in the case of specimens with tubular geometry, both wall thickness and circumference, and in flat specimens both the width and thickness could control the fracture lifetimes.

### 5. SECTION SIZE EFFECT AND FAILURE IN GAS TURBINE ENGINE BLADE

An excellent example of the section effect on creep life is found in the case of a high pressure gas turbine engine blade, forged from Nimonic 108, a nickel base superalloy. The more advanced engines carry blades with a modified design having bull-nosed leading edge containing a cooling channel near leading edge at close proximity to the surface. This redesign was expected to maintain the metal temperature within limits even though the turbine entry temperature was higher. Contrary to this expectation, cracks appeared in a few blades after being in operation barely for 70 h (Fig. 19). The blades always failed at midspan region of the leading edge (Fig. 20). The cracked as well as failed blades were investigated for the cause of failure<sup>25</sup>. The blades were examined by optical and scanning electron microscopy. The wall thickness was measured in all the cracked and failed blades. It was observed that the blade with

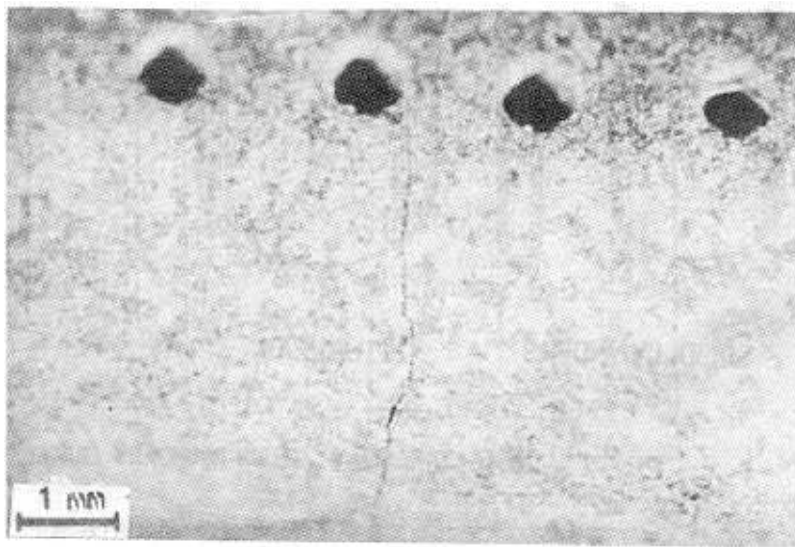


Figure 19. A gas turbine engine blade formed cracks just after 70 h in service.

the minimum wall thickness gave the lowest creep life (Fig. 21). The failure investigation provided evidence that cracks initiated due to thermal fatigue as the blades experienced frequent heating and cooling cycles in service. The growth of these cracks was enhanced by grain boundary oxidation (Fig. 22) until a critical crack length was reached for failure to take place. From this failure investigation, it becomes quite clear that in order to avoid a premature failure of the gas turbine engine blades, a proper understanding of the synergistic effect between section size and oxidation on creep life must be achieved.

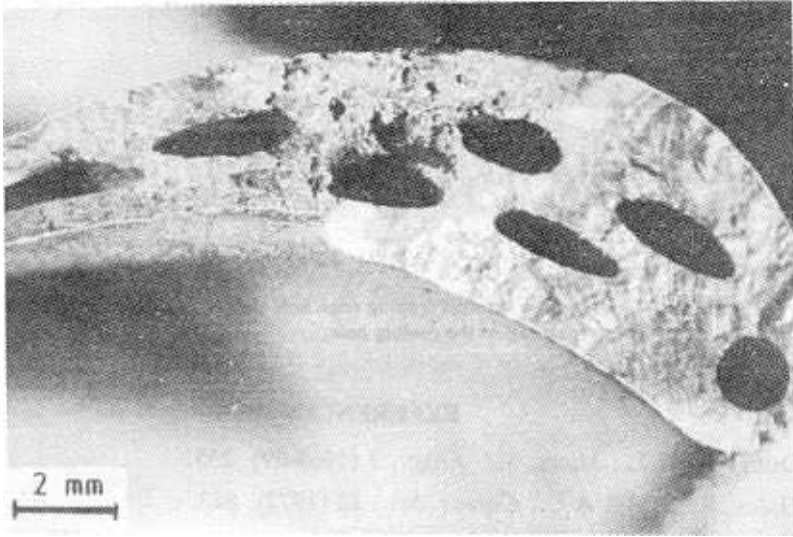


Figure 20. Fracture surface of the blade.

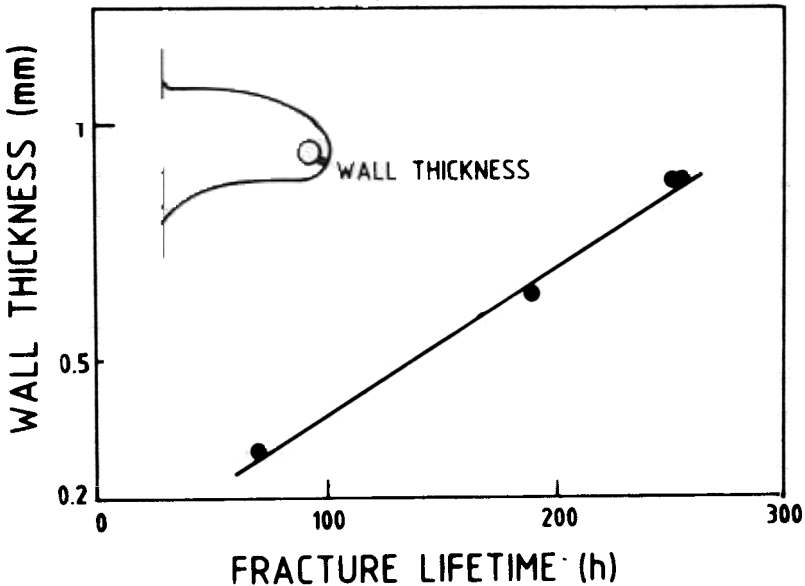


Figure 21. Wall thickness versus fracture lifetime in the gas turbine engine blade.

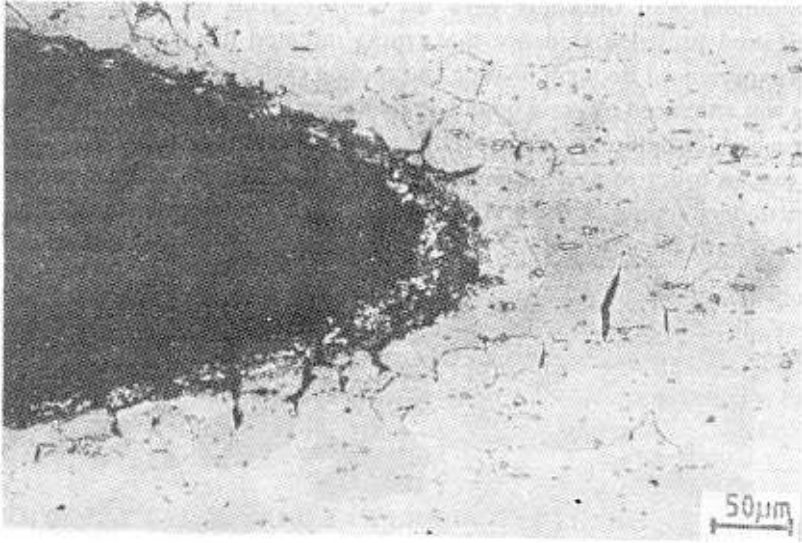


Figure 22. Taper section through leading edge hole showing oxidation and cracking at internal wall of the cooling hole.

#### REFERENCES

1. Douglass, D.L., *Mater. Sci. Engg.*, **3** (1968-69), 255.
2. Hales, R. & Hill A.C., *Corros. Sci.*, **12** (1972), 843.
3. Hancock, P., *Vacancies 76*, (The Metals Society, London), 1976, p. 215.
4. Caplan, D., Hussey, R.J., Sproule, G.I., & Graham, M.J., *Oxid. Metals*, **14** (1980), 279.
5. Harris, J.E., *Acta Metall.*, **26** (1978), 1033.
6. Stringer, J., *Corros. Sci.*, **10** (1970), 513.
7. Lowell, C.E., Grisaffe, S.J. & Deadmore, D.L., *Oxid. Metals*, **4** (1972), 91.
8. Bricknell, R.H. & Woodford, D.A., *In Creep and Fracture of Engineering Materials*, B. Wilshire and D.R.J. Owen, (Eds), (Pineridge Press, Swansea), 1981, p. 249.
9. Bricknell, R.H. & Woodford, D.A., *Acta Metall.*, **30** (1982), 257.
10. Iacocca, R.G. & Woodford, D.A., *Metall. Trans.*, **19A** (1988), 2305.
11. Raj, R., *Acta Metall.*, **30** (1982), 1259.
12. Dyson, B.F., *Acta Metall.*, **30** (1982), 1639.
13. Pandey, M.C. & Rama Rao, P., to be published.
14. Chang, W.H., *Superalloys Processing*, AIME, MCIC-72-10, 1972.
15. Pandey, M.C. & Rama Rao, P., *Scripta Metall.*, **23** (1989), 59.
16. Pandey, M.C. & Rama Rao, P., *Scripta Metall.*, **22** (1988), 1201.
17. Richards, E.G., *J. Inst. Metals*, **96** (1968), 365.

18. Dyson, B.F. & Osgerby, S., *Mater. Sci. Tech.*, **3** (1987), 545.
19. Pandey, M.C., Dyson, B.F. & Taplin, D.M.R., *Proc. Roy. Soc., London, Ser. A*, **399** (1984), 117.
20. Pandey, M.C., Taplin, D.M.R., Ashby, M.F. & Dyson, B.F., *Acta Metall.*, **34** (1986), 2025.
21. Pandey, M.C. & Rama Rao, P., to be published (1990).
22. Gibbons, T.B., *Metals Tech.*, **8** (1981), 472.
23. Oxx, G.D., *In Proceedings Int. Conf. on Creep-Fatigue at Elevated Temperature Application*, (Institute of Mechanical Engineers, London), 1974, E212.
24. Pandey, M.C., Taplin, D.M.R. and Rama Rao, P., *Mater. Sci. Engg.*, **A118** (1989), 33.
25. Sreeram Murthy, A.M., Pandey, M.C. & Bhatia, M.L., (Defence Metallurgical Research Laboratory, Hyderabad), unpublished work, 1989.